Perhaps more important, the transport of O_3 by geostrophic winds and changes in the O_3 concentration can be directly observed; this information should contribute significantly to our understanding of the distribution of human impacts on the O_3 layer. Such data may also make possible the first real determination of an anthropogenic effect on the O_3 layer, as a result of a detailed study of the most sensitive region near 40 km (*10*).

A limb scanner providing temperatures down to the tropopause could be used with a conventional downward-looking temperature sounder to produce considerably improved tropospheric soundings for operational meteorological use. In preliminary calculations, we find that root-mean-square tropospheric temperature errors ($\sim$ 2.5 K) can be reduced by up to a factor of 2.

A similar limb scanner on Nimbus 7 has demonstrated the capability to measure the additional trace gases, H_2O, HNO_3, and NO_2 (*11*). The latter two are the first gases present in the parts-per-billion range to be measured from space.

Thus, infrared limb scanning can provide global observations of the stratosphere and mesosphere with unprecedented vertical resolution, accuracy, and precision. These observations will make possible more quantitative tests of theoretical predictions in those regions and detailed studies of global phenomena such as the interaction of chemistry and dynamics.

JOHN C. GILLE, PAUL L. BAILEY
National Center for Atmospheric Research, Boulder, Colorado 80307
RICHARD A. CRAIG*
Florida State University, Tallahassee 32306
FREDERICK B. HOUSE
Drexel University, Philadelphia, Pennsylvania 19104
GAIL P. ANDERSON
National Center for Atmospheric Research

References and Notes

1. *Halocarbons: Effects on Stratospheric Ozone* (National Academy of Sciences, Washington, D.C., 1976); *Stratospheric Ozone Depletion by Halocarbons: Chemistry and Transport* (National Academy of Sciences, Washington, D.C., 1979).
2. P. J. Ellis, G. Peckham, S. D. Smith, J. T. Houghton, C. G. Morgan, C. D. Rodgers, E. J. Williamson, *Nature (London)* **228**, 139 (1970); M. D. Austen, J. J. Barnett, P. D. Curtis, C. G. Morgan, J. T. Houghton, G. D. Peskett, C. D. Rodgers, E. J. Williamson, *ibid.* **260**, 594 (1976); D. F. Heath, C. L. Mateer, A. J. Krueger, *Pure Appl. Geophys.* **106–108**, 1238 (1973); J. T. Houghton, *Q. J. R. Meteorol. Soc.* **104**, 1 (1978).
3. J. C. Gille, *J. Geophys. Res.* **73**, 1863 (1968).
4. _____ and F. B. House, *J. Atmos. Sci.* **28**, 1427 (1971).
5. J. C. Gille, P. L. Bailey, F. B. House, R. A. Craig, J. R. Thomas, in *Nimbus 6 Users Guide*, J. E. Sissala, Ed. (NASA Goddard Space Flight Center, Greenbelt, Md., 1975), p. 141.
6. P. L. Bailey and J. C. Gille, in *Remote Sensing of the Atmosphere: Inversion Methods and Applications*, A. L. Fymat and V. E. Zuev, Eds. (Elsevier, Amsterdam, 1978), p. 115; F. B. House and J. C. Gille, in preparation; P. L. Bailey and J. C. Gille, in preparation.
7. F. Schmidlin, in preparation.
8. E. Hilsenrath, R. L. Coley, P. T. Kirschner, W. Gammill, *NASA Tech. Mem. 79712* (1979); A. J. Krueger, *Pure Appl. Geophys.* **106–108**, 1272 (1973).
9. I. Hirota, *J. Atmos. Sci.* **36**, 217 (1979).
10. P. J. Crutzen, I. S. A. Isaksen, J. R. McAfee, *J. Geophys. Res.* **83**, 345 (1978).
11. J. M. Russell III and J. C. Gille, *Nimbus 7 Users Guide*, C. Madrid, Ed. (NASA Goddard Space Flight Center, Greenbelt, Md., 1978), p. 263; J. C. Gille, P. L. Bailey, J. M. Russell III, *Philos. Trans. R. Soc. London Ser. A*, in press.

12. We thank the late W. Nordberg for advice in the formative stages of the experiment; the Honeywell staff, especially J. Thomas, J. Bates, R. Blades, and R. Drozewski; and J. Theon, L. Wilson, and the personnel of the Nimbus Project at NASA Goddard Space Flight Center. We thank A. J. Miller, who supplied rocket temperatures, and E. Hilsenrath and A. Krueger, who provided data from chemiluminescent and optical O_3 rockets, respectively, in advance of publication. The program was supported in part by NASA contract NAS5-21652 and work order S 40135B. The National Center for Atmospheric Research is sponsored by the National Science Foundation.

* Richard A. Craig died on 1 September 1978.

30 November 1979; revised 23 January 1980

Corrections in the Pioneer Venus Sounder Probe Gas Chromatographic Analysis of the Lower Venus Atmosphere

Abstract. *Misidentification of two peaks from the Pioneer Venus sounder probe gas chromatograph (SPGC), also formerly known as the LGC, gave rise to quantitative errors in the abundances of oxygen, argon, and carbon monoxide. The argon abundance is estimated at 67 parts per million and that of carbon monoxide at 20 parts per million. At this time, no estimates for the oxygen abundance can be made.*

We reported earlier on the compositional analysis of the lower atmosphere of Venus (*1*). We report here a revised compositional analysis derived from simulation studies and further chromatographic comparison (Table 1). This composition differs from that published earlier because we had misidentified the Ar peak as O_2 and the CO peak as Ar. This consequently gave rise to the quantitative errors because response factors are different for each component analyzed. An equivocal presence of O_2, revised values for Ar, and an estimation of CO (instead of an upper limit in the lower atmosphere of Venus) are shown in Table 1. The misidentifications of peaks were caused by assuming that the retention times were sufficient for identification. This conclusion was reasonable as derived from Table 2, where retention times from the flight data were matched with those of known calibration gas standards obtained before flight. The largest difference was in Freon 14, which had a retention time of 24 seconds less in the flight data than in the calibration tests. We assumed that the temperature of the column rose during the later stages of the third analysis and did not put any credence on the shortened retention time of the added Freons. We have since found that the short retention times for all gases were caused by higher mass flow rates in the column.

We discovered the error after com-

Table 1. Revised atmospheric composition of Venus as measured by the SPGC.

Gas	Flight sample 1	Flight sample 2	Flight sample 3
	*Concentration (%) ± confidence interval**		
CO_2	95.4 ± 2.0	95.9 ± 5.8	96.4 ± 1.0
N_2	4.60 ± 0.14	3.54 ± 0.04	3.41 ± 0.01
H_2O	< 0.06	0.519 ± 0.068	0.135 ± 0.015
	*Concentration (ppm) ± confidence interval**		
O_2	?	?	?
CO	32.2 $^{+61.7}_{-22.2}$	30.2 ± 18.0	19.9 ± 3.1
Ar	60.5 ± 46.8	63.8 ± 13.6	67.2 ± 2.3
Ne	< 8	10.6 $^{+31.6}_{-9.6}$	4.31 $^{+5.54}_{-3.91}$
SO_2	< 600	176 $^{+2000}_{-0}$	185 $^{+350}_{-155}$
Altitude† (km)	51.6	41.7	21.6
Pressure‡ (bars)	0.698 ± 0.140	2.91 ± 0.17	17.8 ± 0.2

*Confidence intervals are calculated from the calibration data acquired during the test and are determined to 3σ (σ is the standard deviation) (*8*). †Altitudes are interpolated from data provided by A. Seiff and represent the altitude at the time of sample injection. ‡Atmospheric pressure at the time of injection as determined by the SPGC from the sum of all measured components.

0036-8075/80/0425-0399$00.50/0

paring the third sample flight chromatogram with a preflight test chromatogram from the flight unit and with a Venus atmospheric simulation chromatogram recently obtained from the flight spare unit. A portion of the three comparative chromatograms with the time base corrected for flow differences is shown in Fig. 1. Thus it is clear that the prior identification based on retention times of the second and third peaks in the flight chromatogram is suspect. Relative retention data shown in Table 3, based on the added Freon standards chosen for each column, verify the conclusion derived from the comparative chromatograms in Fig. 1. The best-fit relative retentions (Table 3) are aligned and confirm the identification of second and third peaks in the flight chromatogram (Fig. 1) as Ar and CO, respectively. The trailing edge of the large N_2 peak obscures direct measurement of low concentrations of O_2 in the third flight chromatogram, whereas the Ar and CO are clearly identifiable and measurable.

In chromatograms obtained from Venus atmospheric samples 1 and 2 (not shown), we see a peaklike feature on the trailing edge of the N_2 peak having a retention time corresponding to O_2. Further simulations and data refinement should resolve the question of whether O_2 is present. At this time we cannot set either a firm value or an upper limit for the O_2 content of the lower atmosphere. Moreover, further studies are required to authenticate O_2 in the chromatograms because O_2 has direct bearing on limiting the concentrations of reduced S species. Small traces of O_2 in the Venus atmosphere may well account for the less than predicted concentration of COS (*2*) and may be incompatible with the presence of elemental S in the clouds.

In an atmosphere containing defined amounts of Ne, Ar, H_2O, CO_2, N_2, CO, and SO_2, the thermodynamic equilibrium mixture, formed at the Venus surface temperature and pressure, results in 5 (*3*) to 20 parts per million (ppm) (*4*) of COS and traces of S_2 and H_2S. The predicted abundance of COS is higher than the 2 ppm reported limit of detectability for this gas by the Pioneer Venus sounder probe gas chromatograph (SPGC). The SPGC has set an upper level for COS which remains to be confirmed in simulation studies.

Our best approximation for Ar is 67.2 ± 2.3 ppm. It is slightly more than the value reported for the Venera 11 gas chromatograph of 40 ± 20 ppm (*5*) but less than the 150 ± 50 ppm reported for the Venera 11 mass spectrometer (*6*); it lies within the errors bars of the Pioneer Venus sounder probe neutral mass spectrometer, 100 ± 80 ppm (*7*). Our approximation for CO is 19.9 ± 3.1 ppm, which compares favorably with the reported 28 ± 14 ppm from the Venera 11 gas chromatograph (*5*).

VANCE I. OYAMA
GLENN C. CARLE
FRITZ WOELLER
NASA Ames Research Center, Moffett Field, California 94035

Table 2. Comparison of retention times (in seconds) of calibration gases and Venus atmospheric constituents. Flight sample components are matched to the closest retention time; S.D., standard deviation.

Gas	Calibration tests ± S.D.	Flight sample		
		1	2	3
	Short column			
Ne	22.85 ± 0.36		22.06	22.44
H_2	24.05 ± 0.47			
N_2	28.51 ± 0.25	26.99	27.16	26.58
Freon 14	40.02 ± 0.15			36.61
CH_4	42.02 ± 0.34			
Kr	42.28 ± 0.38			
CO_2	45 to 68*	60.28	55.91	44.87
N_2O	86.23 ± 1.89			
C_2H_4	122.45 ± 0.64			
C_2H_6	166.90 ± 0.82			
H_2O	175 to 214*		181.21	180.50
H_2S	219.48 ± 0.84			
COS	406.27 ± 2.91			
Freon 22	520.16 ± 0.39			497.71
SO_2	607.79 ± 2.13		592.17	580.81
C_3H_8	764.28 ± 4.46			
	Long column			
Ne	218.42 ± 0.51		217.94	214.01
H_2	231.02 ± 0.47			
N_2	306.76 ± 0.53	300.03	298.98	293.84
O_2	323.14 ± 0.54	326.56	326.08	323.56
Ar	334.24 ± 0.66	337.37	336.12	333.64
CO	345.24 ± 0.93			
CH_4	589.27 ± 0.95			
Freon 14	609.04 ± 0.16			587.87
Kr	646.47 ± 0.94			

*Retention times of CO_2 and H_2O increase over the reported range with decreasing concentrations in the sample.

Table 3. Comparison of the relative retention of calibration gases and constituents of the Venus atmosphere for both the long and short columns. Components are matched to the closest values.

Gas	Calibration test range	Sample 3
	Long column	
Ne	0.358 to 0.359	0.364
H_2	0.378 to 0.380	
N_2	0.502 to 0.505	0.500
O_2	0.529 to 0.531	
Ar	0.547 to 0.550	0.550
CO	0.565 to 0.568	0.568
Freon 14	1.000	1.000
Kr	1.059 to 1.063	
	Short column	
Ne	0.043 to 0.045	0.45
H_2	0.045 to 0.047	
N_2	0.054 to 0.055	0.053
Freon 14	0.076 to 0.077	0.074
CO_2	0.086 to 0.130	0.090
H_2O	0.34 to 0.41	0.36
Freon 22	1.000	1.000
SO_2	1.16 to 1.17	1.166

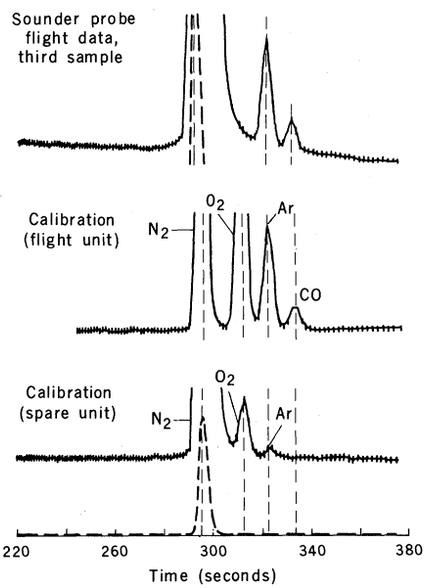

Fig. 1. Comparative chromatograms.

References and Notes

1. V. I. Oyama, G. C. Carle, F. Woeller, J. B. Pollack, *Science* **203**, 802 (1979); *ibid.* **205**, 52 (1979).
2. R. G. Prinn, *Geophys. Res. Lett.* **6**, 808 (1979).
3. R. Craig and R. Reynolds, personal communication (results of thermodynamic equilibrium calculations based on the SPGC composition at al-

titudes of 40 to 45 km extrapolated to surface conditions).
4. V. A. Krasnopolsky and V. A. Parshev, personal communication (model thermodynamic equilibrium calculations from Venera data).
5. B. G. Geljman *et al.*, *Astrophys. J.* **5**, 217 (1979).
6. V. G. Isotomin, K. V. Grechnev, V. A. Kochnev, *ibid.*, p. 211.
7. J. H. Hoffman, R. R. Hodges, Jr., M. B. McElroy, T. M. Donohue, M. Kolpin, *Science* **205**, 49 (1979).
8. M. G. Natrella, *Experimental Statistics* (Handbook 91, National Bureau of Standards, Washington, D.C., 1966), pp. 5-27 to 5-46.

6 December 1979; revised 29 January 1980

Enhancement of Superconductivity through Lattice Softening

Abstract. *The superconducting transition temperature of an iridium-yttrium eutectic is enhanced extraordinarily through lattice softening. This is shown by a drastically reduced Debye temperature.*

Iridium is a superconductor at 0.10 K (*1*). The eutectic formed by iridium with neighboring phases such as YIr_2 or $EuIr_2$ is a bulk superconductor with superconducting transition temperatures (T_c) ranging from 2.7 to 3.7 K. Neither YIr_2 nor $EuIr_2$ by itself is superconducting above 1 K. The T_c of $EuIr_2$ was found at 0.2 K (*2*), and that of YIr_2, apart from superconducting traces, is probably not above 20 mK (*3*). It has long been known that the addition of merely 1 atom percent yttrium will lead to inductive and resistive superconducting transitions above 3 K. However, this result had been considered due to the presence of a hypothetical second phase with the approximate composition IY : 4Ir. Actually, yttrium and europium were not the only rare earth elements leading to a superconducting iridium eutectic; lanthanum and cerium had previously shown a similar behavior (*4*). We have now ascertained that the superconductivity observed is due to the eutectic proper and no other spurious or new phase is involved.

Measurements of the Debye temperature θ_D show a spectacular drop from 420 K for pure iridium to 175 K near the eutectoid composition at about 22 atom percent Y. The system Ir-Y was chosen for the complete study because of the absence of significant second-phase formation for compositions as rich in Y as $Ir_{0.9}Y_{0.1}$ as well as the absence of superconductivity of YIr_2 above 20 mK. Previous results to the contrary must have been due to stoichiometric deficiencies (*4*). It is now apparent, and supported by metallography and transmission electron microscopy, that the enhanced bulk superconductivity of the eutectic is caused by the microscopic mixture of Ir with small amounts of YIr_2. This result is supported further by our specific heat measurements (Fig. 1), coupled with Debye-Scherrer x-ray powder patterns. Accordingly, these x-ray results indicate that $Ir_{0.90}Y_{0.10}$ is at least 95 percent single-phase cubic Ir, with a lattice parameter of $a_0 = 3.8389 \pm 0.0004$ Å; $Ir_{0.99}Y_{0.01}$ has $a_0 = 3.8395$ Å, while pure Ir has $a_0 = 3.8389$ Å. This shows that far less than 1 percent Y is soluble in Ir and that the excess Y does not enter the Ir lattice, since a_0 is virtually unchanged, or form enough of a crystalline second phase to account for more than a small fraction of the Y present. The small amount of Y that dissolves in the Ir does not affect the T_c of the Ir. Inductive measurements show the Ir transition to remain at 0.10 K.

The specific heat measurements together with the x-ray results allow no other conclusion than that the microscopic mixture of Ir and YIr_2 in the eutectic phase causes the eutectic to become a bulk conductor at 3.7 K, since the specific heat anomaly only near the eutectic composition indicates essentially a bulk effect. This microscopic mixture has such small grains of crystallinity that they are not seen in the x-ray patterns on unannealed, arc-melted samples. Furthermore, rapid quenching of the samples seems to adversely affect the superconductivity. Transmission electron microscopy reveals the classical picture of a lamellar eutectic (Fig. 2).

To shed some light on the phenomenon that the eutectic shows a superconducting transition enhanced by at least a factor of 30 over that of iridium, the element, it is of great interest to compare the specific heat measurements. In Fig. 1, lattice specific heat (θ_D) and electronic specific heat (γ) are shown as

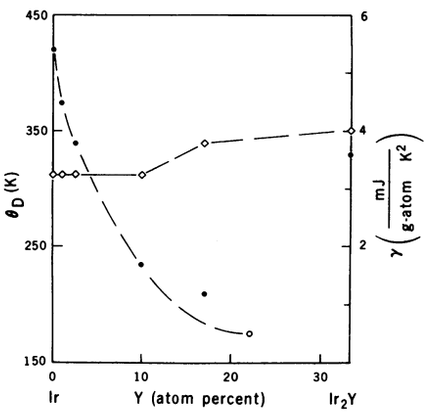

Fig. 1. (●, ○) Debye temperature θ_D and (◇) electronic specific heat term γ for Ir-Y alloys. The open circle is an extrapolated point.

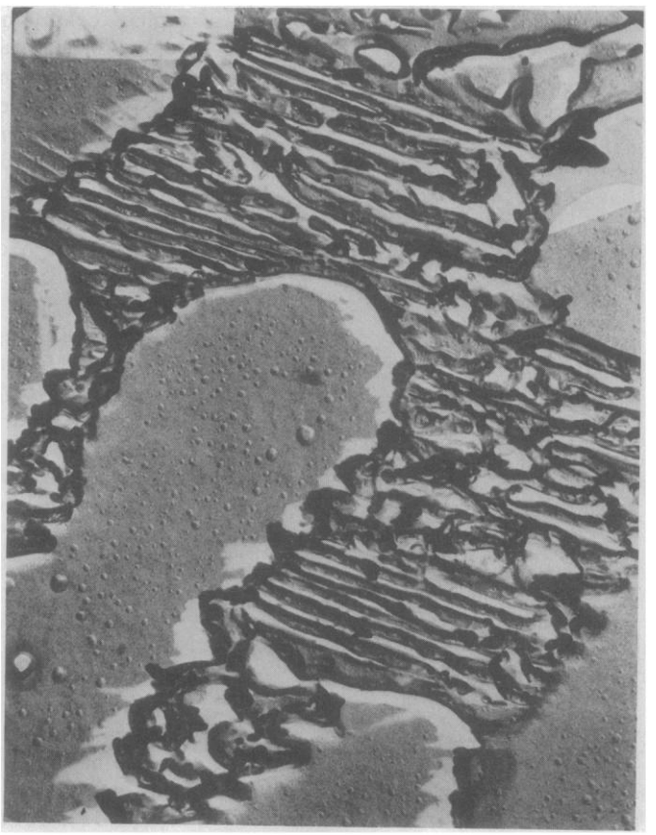

Fig. 2. Transmission electron microscopy replica of $Ir_{0.95}Y_{0.05}$ showing the lamellar eutectic together with elemental iridium (×24,000).

0036-8075/80/0425-0401$00.50/0